

# PROMPT WHEN THE ANIMAL IS: TEMPORAL ANIMAL BEHAVIOR GROUNDING WITH POSITIONAL RECOVERY TRAINING

Sheng Yan<sup>1</sup>, Xin Du<sup>1</sup>, Zongying Li<sup>1</sup>, Yi Wang<sup>1</sup>, Hongcang Jin<sup>1</sup>, Mengyuan Liu<sup>2,†</sup>

<sup>1</sup>School of Artificial Intelligence, Chongqing University of Technology

<sup>2</sup>National Key Laboratory of General Artificial Intelligence, Shenzhen Graduate School, Peking University

## ABSTRACT

Temporal grounding is crucial in multimodal learning, but it poses challenges when applied to animal behavior data due to the sparsity and uniform distribution of moments. To address these challenges, we propose a novel Positional Recovery Training framework (Port), which prompts the model with the start and end times of specific animal behaviors during training. Specifically, Port enhances the baseline model with a Recovering part to predict flipped label sequences and align distributions with a Dual-alignment method. This allows the model to focus on specific temporal regions prompted by ground-truth information. Extensive experiments on the Animal Kingdom dataset demonstrate the effectiveness of Port, achieving an IoU@0.3 of 38.52. It emerges as one of the top performers in the sub-track of MMVRAC in ICME 2024 Grand Challenges.

**Index Terms**— Temporal Grounding, Animal Kingdom, Multi-modal Learning, Deep Learning

## 1. INTRODUCTION

Temporal grounding, a crucial task in multimodal learning [1, 2, 3, 4, 5, 6, 7, 8, 9, 10, 11], involves retrieving or localizing target moments that semantically correspond to given language queries. Recent literature [12] indicates that despite the commendable performance of representative works such as VSLNet [1] and LGI [13] on conventional temporal grounding benchmarks [14, 2], they fall short when applied to animal behavior data [12]. We attribute this primarily to discrepancies in the sparsity of moments and their temporal position distribution:

① In the wild, capturing valuable footage of animals requires enduring long periods of waiting, where each captivating moment may vanish in an instant. This results in recorded videos containing only a fraction of animal footage or possibly none at all. In fact, as shown in Table 1, we list the Animal Kingdom dataset for animal behavior localization alongside the average moment, average duration, and the normalized moment length  $\bar{L}_{m/v}$  relative to the length of the

Dataset	$\bar{L}_{video}$	$\bar{L}_{moment}$	$\bar{L}_{m/v}$
Charades-STA [2]	30.59s	8.22s	0.27
ActivityNet Captions [14]	117.61s	36.18s	0.32
Animal Kingdom [12]	38.15s	6.27s	0.19

**Table 1.** Statistics of temporal grounding datasets, where  $\bar{L}_{video}$ ,  $\bar{L}_{moment}$  denotes the average length of videos, temporal moments in seconds, and  $\bar{L}_{m/v}$  is the normalized moment length, against video length.

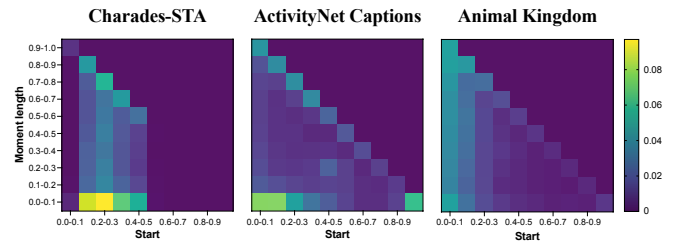


**Fig. 1.** Distribution of temporal positions of target moments: Conventional grounding benchmarks VS. Animal Kingdom dataset. The color gradient indicates the relative frequency, with brighter shades indicating higher proportions.

source video. As can be seen, Animal Kingdom’s normalized moment length is only 0.19, which is a smaller characteristic when compared to traditional localization benchmarks [14, 2]. Because of temporal sparsity, the shorter normalized length suggests difficulties with moment retrieval [15].

② The heatmaps in Fig. 1 illustrate the overall distribution of temporal moment positions between conventional temporal grounding benchmarks [14, 2] and Animal Kingdom [12]. Here, the horizontal and vertical axes represent the starting time and duration of moments, respectively, normalized to the range of 0 to 1 by dividing them by the corresponding video lengths. Each grid cell denotes the corresponding percentage. In Charades-STA, target moments are more likely to start from the beginning of the video and last for approximately 10% of the video length. For ActivityNet Captions, a peak can be observed near the bottom left corner of the graph. This peak corresponds to moments starting from the beginning of the video, also covering around 10% of the video length. These biases provide strong priors for moment

† Corresponding author: Mengyuan Liu (liumengyuan@pku.edu.cn).

positions. Weighting candidate positions based on these distributions can increase the chances of obtaining the correct moments on conventional benchmarks [16]. However, such positional biases are significantly subtle in Animal Kingdom, as its distribution is more uniform (none of the grid cells exhibit bright green or yellow). Consequently, models benefiting from these positional biases [1, 13, 17] exhibit weakened capabilities.

To overcome the impact of the aforementioned moment disparities, we contemplate whether prompting the model with the starting or ending times of a certain animal behavior during training could focus the model’s attention on that region. To this end, we propose a Positional Recovery Training framework, inspired by recent works that injecting ground-truth information into object detection networks [18, 19, 20]. Specifically, building upon the classical proposal-free framework, VSLNet [1], we significantly enhance its final predictor. We divide the predictor into two parts. In addition to the *Predicting part*, which can predict the distribution of starting/ending boundaries of target moments normally, a *Recovering part* is introduced in parallel to perform positional recovery training. In this part, our goal is to recover the flipped starting/ending label sequences. Since these sequences are already close to the ground truth, learning in this part is easier and the predicted distributions are more accurate. Subsequently, a *Dual-alignment* method is employed to force the distributions of the predicting part to overlap with them. This method prompts the Recovering part to suggest the starting or ending times corresponding to a certain animal behavior to the Predicting part.

Extensive experiments demonstrate that executing positional recovery training is effective. The proposed framework termed as `Port`, which stands for Temporal Animal Behavior Grounding with Positional Recovery Training, achieves outstanding performance on the Animal Kingdom dataset with  $\text{IoU}@0.3=38.52$ . Moreover, it has been selected as one of the top performers in the Multi-Modal Video Reasoning and Analyzing Competition (MMVRAC) – Track 5: Video Grounding<sup>1</sup> at the International Conference on Multimedia and Expo in 2024.

## 2. PRELIMINARY

In this paper, we adopt a subclass of proposal-free frameworks called Span-based prediction methods, which directly predict the probability of each video frame being the start/end position of a target moment. Next, we provide the definition of this task:

**Video and Text query.** A video is defined as a sequence of untrimmed frames,  $\mathbf{V} \in \mathbb{R}^{T \times d_v}$ , taken from a 3D ConvNet pre-trained on the Kinetics dataset [21], using RGB visual feature extraction and subsampling. For textual queries, they describe the target moment. This description contains precise

animal behavior, such as “*The bird dips its face into the water.*” The data structure is a word sequence  $\mathbf{Q} \in \mathbb{R}^{N \times d_w}$  of length  $N$ , where  $d_w$  represents the word embedding dimension, indicating 300d GloVe vectors [22].

**Task objective.** Given a video  $\mathbf{V}$  and a textual query  $\mathbf{Q}$  describing the target moment, where  $\tau_s$  and  $\tau_e$  represent the ground-truth starting and ending time points, respectively. Span-based method aims to predict the starting and ending boundaries of the target moment span. Thus, it is necessary to map the starting/ending time  $\tau_{s(e)}$  to the corresponding indices  $i_{s(e)}$  in the video sequence  $\mathbf{V}$ . Specifically, assuming the video duration is  $\mathcal{T}$ , the computation formula for the starting/ending indices  $i_{s(e)}$  is:  $i_{s(e)} = \langle \tau_{s(e)} / \mathcal{T} \times T \rangle$ , where  $\langle \cdot \rangle$  denotes the rounding operator. Given a pair  $(\mathbf{V}, \mathbf{Q})$  as input, Span-based method locates the time span from the starting  $i_s$  to the ending  $i_e$ . During inference, the predicted span boundaries can be easily converted to the corresponding times using  $\tau_{s(e)} = i_{s(e)} / T \times \mathcal{T}$ .

## 3. METHOD

### 3.1. VSLNet Baseline

Our model is built upon VSLNet [1], which treats the video as a text passage, the target moment as the answer span, and adapts a multimodal span-based question answering (QA) framework to the temporal grounding task. This architecture follows the “encode-fuse-highlight-predict” paradigm (see Fig. 2 for an overview). Next, we briefly review the components of VSLNet and the training loss.

**Multi-modal learning.** The key components of this framework include the Feature Encoder, Context-Query Attention, and Conditional Span Predictor. The Feature Encoder utilizes a simplified version of the QANet [23] embedding encoder layer to project visual and textual features into a shared dimension. The Context-Query Attention captures cross-modal interactions between visual and textual features, which are crucial for understanding the video content within the context of the textual query. The Conditional Span Predictor is constructed based on a unidirectional LSTM and FFN layers to predict the starting and ending boundaries of answer spans in the video. Additionally, VSLNet introduces Query-Guided Highlighting (QGH) to enhance performance. QGH extends the boundaries of the target moment in the video, incorporating additional contextual information to aid in predicting the answer span. This binary classification module predicts the confidence of each visual feature belonging to the foreground or background.

To establish a solid baseline, in our framework, we adopt the subsequent work of VSLNet, self-guided parallel attention (SGPA) [24], as our Feature Encoder. Moreover, we omit the extension of boundary in the QGH strategy. We note that these improvements are effective in enhancing the encoding effectiveness.

**VSLNet losses.** We keep the same base set of losses of [1],

<sup>1</sup><https://sutdvcv.github.io/MMVRAC/>

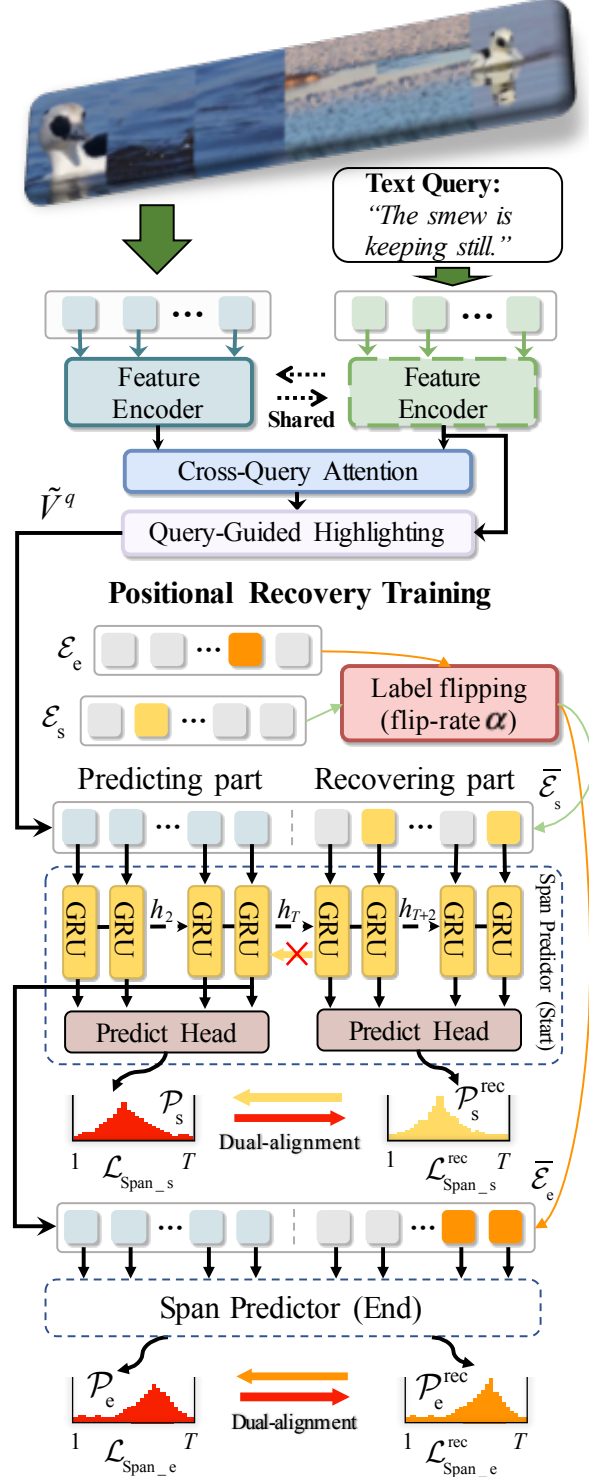


**Fig. 2.** Our proposed PORT is built upon VSLNet. We significantly improve the predictor through Positional Recovery Training. We divide the predictor into two parts: the Predicting part and the Recovering part. Both parts share the same optimization objective, but the Recovering part conducts recovery training on the flipped embedded sequences  $\tilde{\mathcal{E}}_{s/e}$  (composed of start (yellow)/non-start (grey) or end (orange)/non-end label embeddings).

defined as the weighted sum  $\mathcal{L}_{\text{VSLNet}} = \mathcal{L}_{\text{span}} + \lambda_{\text{QGH}} \mathcal{L}_{\text{QGH}}$ . In summary, the span prediction loss term  $\mathcal{L}_{\text{span}}$  measures the difference between the predicted probability distributions of the starting and ending boundaries (via a cross-entropy loss). The QGH loss term  $\mathcal{L}_{\text{QGH}}$  is related to the QGH strategy, which emphasizes highlighting relevant video features based on the input query. The loss is computed based on a binary classification task of predicting whether the visual features belong to the foreground (i.e., target moment) or background (with a binary cross-entropy loss). We set  $\lambda_{\text{QGH}}$  to 5.0 in our experiments, as in [1].

### 3.2. Positional Recovery Training

We have significantly improved the predictor of the baseline model to overcome the effects of moment disparities analyzed in the introduction. Specifically, we divide LP-Predictor into two parts: *Predicting part* and *Recovering part*. In the first part, the predictor predicts the distribution of start/end boundaries normally. In the second part, we train to recover the flipped start/end label prior sequences. Then, we use a *Dual-alignment* method to force the predicted distributions of the Predicting part to overlap with them. Below, we will detail the prediction of start boundaries as an example.

**Predicting part.** The Span Predictor (Start) consists of a unidirectional *GRU* and a Predict Head, where the head is a 2-layer *FFN* network with *LayerNorm* and *ReLU* activation. The score for the start boundary is computed as follows:

$$\mathcal{S}_s = \text{PredHead}(\mathbf{V}_s^q), \mathbf{V}_s^q = \text{GRU}(\tilde{\mathbf{V}}^q) \quad (1)$$

where  $\mathcal{S}_s \in \mathbb{R}^T$ ;  $\tilde{\mathbf{V}}^q \in \mathbb{R}^{T \times d}$  represents the query-highlighted features, weighted by the QGH strategy, and then the probability distribution for start boundaries is calculated by  $\mathcal{P}_s = \text{Softmax}(\mathcal{S}_s)$ . The training objective is:

$$\mathcal{L}_{\text{Span}_s} = f_{\text{CE}}(\mathcal{P}_s, \mathcal{Y}_s) \quad (2)$$

where  $\mathcal{Y}_s$  represents the labels for the starting boundary.  $f_{\text{CE}}$  is the cross-entropy function.

**Recovering part.** In this part, we first embed the start label sequences  $\mathcal{Y}_s \rightarrow \mathcal{E}_s \in \mathbb{R}^{T \times d}$ . For these sequences, we apply *Label flipping*, meaning that we randomly swap start labels with non-start labels within the sequence. We have a hyperparameter  $\alpha$  to control the rate of flipping, and the flipped sequence can be represented as  $\tilde{\mathcal{E}}_s$ . Subsequently, we concatenate it with the highlighted feature  $\tilde{\mathbf{V}}^q$  and fed to the Span Predictor (Start) together, as illustrated in Fig. 2-middle. Our goal is to recover  $\tilde{\mathcal{E}}_s$  back to  $\mathcal{E}_s$  by comprehending the hidden state  $h_T$  passed by the *GRU* (i.e., sequence-level highlighted feature). Consequently, a cross-entropy loss is used to optimize the recovery process:

$$\mathcal{L}_{\text{Span}_s}^{\text{rec}} = f_{\text{CE}}(\mathcal{P}_s^{\text{rec}}, \mathcal{Y}_s) \quad (3)$$

where  $\mathcal{P}_s^{\text{rec}} \in \mathbb{R}^T$  is the predicted start boundary distribution for this part, obtained by softmaxing the scores. Intuitively,

**Table 2.** Results on the Animal Kingdom test split.

Method	IoU=0.3	IoU=0.5	IoU=0.7	mIoU
LGI [13]	33.51	19.74	8.94	22.90
VSLNet [1]	33.74	20.83	12.22	25.02
Port (Ours)	<b>38.52</b>	<b>26.41</b>	<b>15.87</b>	<b>28.10</b>

the forward process of the Recovering part is parallel to the Predicting part

Note that the *GRU* is set to be unidirectional, ensuring that the Recovering part does not leak ground-truth information to the Predicting part.

**Dual-alignment.** In contrast to the Predicting part, the learning in the Recovering part is relatively easier, and the predicted distribution is more accurate because we only slightly flip the label sequences. To enforce the predictions of the Predicting part to be as close as possible to the Recovering part, we minimize the Kullback-Leibler (KL) divergence between the distributions  $\mathcal{P}_s$  and  $\mathcal{P}_s^{\text{rec}}$ :

$$\mathcal{L}_{\text{Align}} = D_{\text{KL}}(\mathcal{P}_s || \mathcal{P}_s^{\text{rec}}) \quad (4)$$

Similarly, this is done for the prediction of the end boundary, with the only difference being conditioned on the start boundary (as shown in Fig. 2-bottom).

**Training loss.** The total loss used to train `Port` is a weighted sum  $\mathcal{L}_{\text{VSLNet}} + \lambda_{\text{Recovering}} \mathcal{L}_{\text{Span}}^{\text{rec}} + \lambda_{\text{Align}} \mathcal{L}_{\text{Align}}$ , where  $\mathcal{L}_{\text{Span}}^{\text{rec}} = \mathcal{L}_{\text{Span}_s}^{\text{rec}} + \mathcal{L}_{\text{Span}_e}^{\text{rec}}$ ;  $\lambda_{\text{Recovering}}$  and  $\lambda_{\text{Align}}$  control the importance of the positional recovery training.

## 4. EXPERIMENT

### 4.1. Experiment Setting

**Animal Kingdom** [12] provides frame-level natural language descriptions of wildlife behavior. It includes various wildlife species, such as whooper and hornbill, sourced from YouTube and ensured for quality through multiple rounds of inspection. The dataset comprises a total of 50 hours of video (across 4301 long video sequences) and 18,744 annotated sentences. Each video sequence contains 3-5 sentences. The dataset is divided into a training set (3489 video sequences and 14,995 text descriptions) and a test set (812 video sequences and 3749 text descriptions) in an 8:2 ratio.

**Evaluation protocol.** We adopt “IoU =  $\mu$ ” and “mIoU” as evaluation metrics [2]. “IoU =  $\mu$ ” indicates the percentage of language queries with at least one retrieved moment having an Intersection over Union (IoU) greater than  $\mu$  with the ground truth. “mIoU” represents the average IoU across all test samples. In our experiments, we use  $\mu \in \{0.3, 0.5, 0.7\}$  and retrieve the moments with the maximum joint probability of starting/ending boundaries (Eq. 2) generated from boundary transformations mentioned in Sec. 2 (i.e., Recall@1).

**Implementation Details.** We use the AdamW optimizer to guide the optimization process with a batch size of 16 and a

**Table 3.** Ablation study of Positional Recovery Training (PRT).

Method	IoU=0.5	IoU=0.7	mIoU
Port	26.41	15.87	28.10
w/o Dual-alignment	25.37	15.52	26.91
w/o PRT	24.97	15.39	27.16

**Table 4.** Ablation study of Positional Encoding.

Position encoding	IoU=0.5	IoU=0.7	mIoU
Learned embeddings	24.72	13.77	26.54
Sinusoidal encoding	25.42	14.49	26.25
None	26.41	15.87	28.10

weight decay parameter of 0.01. The model training process spans 100 epochs, with an initial learning rate of  $2e - 4$  linearly decayed. We set the maximum video length  $T$  to 128 and the model’s hidden dimension  $d$  to 256. The flip rate  $\alpha$  for positional recovery training is set to 0.2. The loss balancing parameters  $\lambda_{\text{Recovering}}$  and  $\lambda_{\text{Align}}$  are both set to 1.0. All experiments are conducted on a single NVIDIA RTX 4090.

### 4.2. Quantitative Results

We compare `Port` with existing methods documented in the literature, including LGI [13] and VSLNet [1]. As shown in Table 2, the best performance is highlighted in **bold**. Thanks to positional recovery training, i.e., by prompting the model with the start/end times of animal behaviors, our `Port` achieves the best performance.

### 4.3. Ablation Study

**Ablation on Positional Recovery Training (PRT).** Table 3 presents the results without Dual-alignment (abbreviated as *w/o Dual-alignment*) and without Positional Recovery Training (*w/o PRT*). When *w/o PRT*, our model degenerates into the VSLNet baseline. The ablation results indicate the effectiveness of our PRT (26.41 vs. 24.97 at IoU@0.5). An interesting observation is that the difference between the results of *w/o Dual-alignment* and *w/o PRT* is not significant. This suggests that the Dual-alignment method is crucial for PRT, indicating that PRT only works effectively through this method after prompting the model with start/end times.

**Is positional encoding all you need?** We examined the descriptions of animal behaviors and found them to be shorter than those of conventional localization benchmarks. Importantly, they rarely include words depicting temporal relationships, such as ‘before’ or ‘after’. We speculate that strong temporal relationship modeling may be weakly correlated with Animal Kingdom. Therefore, we experimented with removing positional encodings and compared them with learnable and sine positional encodings. Table 4 shows that no positional encoding is more suitable for temporal animal behavior grounding.

**Table 5.** Ablation on various model hidden size ( $d$ )

Hidden dim	IoU=0.5	IoU=0.7	mIoU
$d = 128$	24.94	15.26	27.77
$d = 256$	26.41	15.87	28.10
$d = 384$	25.50	15.26	26.87
$d = 512$	25.45	15.82	26.96

**Which hidden dim is the best?** The results in Table 5 demonstrate that the performance is optimal when the hidden dimension  $d$  of the model is set to 256.

Text Query: The archer fish is swimming.



Ground Truth	10.8s	- - - - - >	13.6s
VSLNet	IoU: 77.3%	10.7s	- - - - - >   13.1s
Port	IoU: 93.7%	10.7s	- - - - - >   13.6s

Text Query: The bird is swimming.



Ground Truth	19.9s	- - - >	26.0s	
VSLNet	14.0s	- - - - >	26.0s	IoU: 50.1%
Port	20.5s	- - - >	29.5s	IoU: 57.3%

Text Query: The hornbill is flying.



Ground Truth	30.9s	- - >	33.4s	
VSLNet	30.9s	- - >	33.0s	IoU: 85.3%
Port	30.9s	- - >	33.6s	IoU: 98.12%

Text Query: The common snipe is walking.



Ground Truth	3.9s	- - - - - >	10.5s	
	0.9s	IoU: 68.5%	- - - - - >	10.6s
	2.4s	IoU: 80.6%	- - - - - >	10.6s

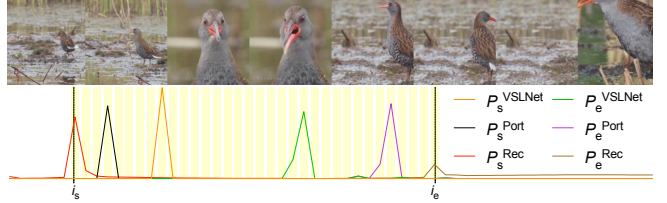
**Fig. 3.** Visualization of the ground-truth moment and predictions by competitor.

#### 4.4. Qualitative Results

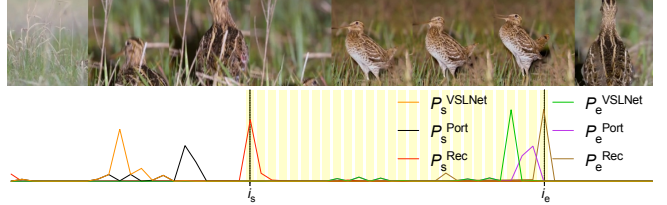
We visualize some qualitative results and compare Port with VSLNet. The results are shown in Fig. 3. Regardless of short or long videos ( $>30s$ ), our Port achieves higher IoU. However, our method also has limitations. In the second case, our model only achieves a 57% IoU. For long videos, our method is currently unstable. This instability arises because in our experiments, long videos are compressed to a fixed length of 128. In this scenario, even small variations in the localized span indices can result in significant changes in the corresponding times after transformation.

Furthermore, we visualize the predicted distributions of the Predicting part and the Recovering part in Port. As shown in Fig. 4, the start and end probabilities of these two

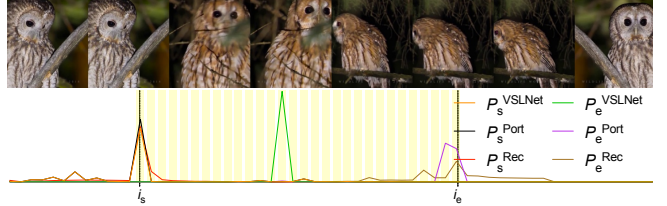
Text Query: The water rail bid is chirping.



Text Query: The great snipe is sensing its environment.



Text Query: The tawny owl is sensing its environment.



Text Query: The tomato frog is eating.

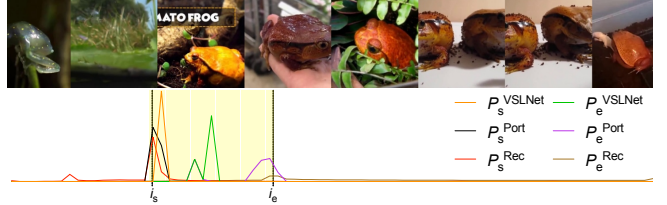


**Fig. 4.** Visualization of the predicted distributions of the Predicting part and the Recovering part in Port, compared to the predicted distribution of VSLNet, with the moment regions highlighted in yellow.

parts are represented as  $P_{s/e}^{Port}$  and  $P_{s/e}^{Rec}$ , respectively, corresponding to the symbols  $\mathcal{P}_{s/e}$  (Eq. 2) and  $\mathcal{P}_{s/e}^{rec}$  (Eq. 3) in the formulas. We compare them with the start and end probabilities of the VSLNet,  $P_{s/e}^{VSLNet}$ . The four cases in Fig. 4 first demonstrate that the peaks of the Recovering part distribution are very close to the start or end indices  $i_{s/e}$  because we only perform slight label flipping, making this part of the learning easy and the predicted distribution accurate. Secondly, compared to the predicted distribution of VSLNet, the predicted distribution of the Predicting part in Port is closer to the distribution of the Recovering part. This demonstrates that Positional Recovery Training helps the model focus on the start/end regions, leading to more accurate grounding results.

## 5. CONCLUSION

In this study, we investigated the emerging problem of temporal animal behavior grounding. We analyzed its discrepancies from conventional temporal grounding benchmarks, which are reflected in the sparsity and uniform distribution of temporal positions. To address this, we proposed the Posi-

tional Recovery Training framework (PORT), which bridges this gap effectively by prompting the model with start and end times of certain animal behaviors.

In future work, we may consider leveraging LLM to identify the subject animals of the moments and adding a classification branch network to enhance model robustness.

## 6. ACKNOWLEDGEMENT

This work was supported by National Natural Science Foundation of China (No. 62203476), Natural Science Foundation of Shenzhen (No. JCYJ20230807120801002).

## 7. REFERENCES

- [1] Hao Zhang, Aixin Sun, Wei Jing, and Joey Tianyi Zhou, “Span-based localizing network for natural language video localization,” *arXiv preprint arXiv:2004.13931*, 2020.
- [2] Jiyang Gao, Chen Sun, Zhenheng Yang, and Ram Nevatia, “Tall: Temporal activity localization via language query,” in *Proceedings of the IEEE international conference on computer vision*, 2017, pp. 5267–5275.
- [3] Chao Guo, Daizong Liu, and Pan Zhou, “A hybrid alignment loss for temporal moment localization with natural language,” in *2022 IEEE International Conference on Multimedia and Expo (ICME)*. IEEE, 2022, pp. 1–6.
- [4] Wen Wang, Ling Zhong, Guang Gao, Minhong Wan, and Jason Gu, “Chan: Cross-modal hybrid attention network for temporal language grounding in videos,” in *2023 IEEE International Conference on Multimedia and Expo (ICME)*. IEEE, 2023, pp. 1499–1504.
- [5] Jueqi Wei, Yuanwu Xu, Mohan Chen, Yuejie Zhang, Rui Feng, and Shang Gao, “Conditional video-text reconstruction network with cauchy mask for weakly supervised temporal sentence grounding,” in *2023 IEEE International Conference on Multimedia and Expo (ICME)*. IEEE, 2023, pp. 1511–1516.
- [6] Zezhong Lv and Bing Su, “Temporal-enhanced cross-modality fusion network for video sentence grounding,” in *2023 IEEE International Conference on Multimedia and Expo (ICME)*. IEEE, 2023, pp. 1487–1492.
- [7] Zongying Li, Yong Wang, Xin Du, Can Wang, Reinhard Koch, and Mengyuan Liu, “Asmnet: Action and style-conditioned motion generative network for 3d human motion generation,” *Cyborg and Bionic Systems*, vol. 5, pp. 0090, 2024.
- [8] Mengyi Zhao, Mengyuan Liu, Bin Ren, Shuling Dai, and Nicu Sebe, “Denoising diffusion probabilistic models for action-conditioned 3d motion generation,” in *ICASSP 2024-2024 IEEE International Conference on Acoustics, Speech and Signal Processing (ICASSP)*. IEEE, 2024, pp. 4225–4229.
- [9] Sheng Yan, Yang Liu, Haoqiang Wang, Xin Du, Mengyuan Liu, and Hong Liu, “Cross-modal retrieval for motion and text via droptriple loss,” in *Proceedings of the 5th ACM International Conference on Multimedia in Asia*, 2023, pp. 1–7.
- [10] Kian Eng Ong, Xun Long Ng, Yanchao Li, Wenjie Ai, Kuangyi Zhao, Si Yong Yeo, and Jun Liu, “Chaotic world: A large and challenging benchmark for human behavior understanding in chaotic events,” in *Proceedings of the IEEE/CVF International Conference on Computer Vision*, 2023, pp. 20213–20223.
- [11] Li Xu and Jun Liu, “Experts collaboration learning for continual multi-modal reasoning,” *IEEE Transactions on Image Processing*, 2023.
- [12] Xun Long Ng, Kian Eng Ong, Qichen Zheng, Yun Ni, Si Yong Yeo, and Jun Liu, “Animal kingdom: A large and diverse dataset for animal behavior understanding,” in *Proceedings of the IEEE/CVF Conference on Computer Vision and Pattern Recognition*, 2022, pp. 19023–19034.
- [13] Jonghwan Mun, Minsu Cho, and Bohyung Han, “Local-global video-text interactions for temporal grounding,” in *Proceedings of the IEEE/CVF Conference on Computer Vision and Pattern Recognition*, 2020, pp. 10810–10819.
- [14] Ranjay Krishna, Kenji Hata, Frederic Ren, Li Fei-Fei, and Juan Carlos Niebles, “Dense-captioning events in videos,” in *Proceedings of the IEEE international conference on computer vision*, 2017, pp. 706–715.
- [15] Hao Zhang, Aixin Sun, Wei Jing, Liangli Zhen, Joey Tianyi Zhou, and Rick Siow Mong Goh, “Natural language video localization: A revisit in span-based question answering framework,” *IEEE transactions on pattern analysis and machine intelligence*, vol. 44, no. 8, pp. 4252–4266, 2021.
- [16] Mayu Otani, Yuta Nakashima, Esa Rahtu, and Janne Heikkilä, “Uncovering hidden challenges in query-based video moment retrieval,” *arXiv preprint arXiv:2009.00325*, 2020.
- [17] Songyang Zhang, Houwen Peng, Jianlong Fu, and Jiebo Luo, “Learning 2d temporal adjacent networks for moment localization with natural language,” in *Proceedings of the AAAI Conference on Artificial Intelligence*, 2020, vol. 34, pp. 12870–12877.
- [18] Nicolas Carion, Francisco Massa, Gabriel Synnaeve, Nicolas Usunier, Alexander Kirillov, and Sergey Zagoruyko, “End-to-end object detection with transformers,” in *European conference on computer vision*. Springer, 2020, pp. 213–229.
- [19] Hao Zhang, Feng Li, Shilong Liu, Lei Zhang, Hang Su, Jun Zhu, Lionel M Ni, and Heung-Yeung Shum, “Dino: Detr with improved denoising anchor boxes for end-to-end object detection,” *arXiv preprint arXiv:2203.03605*, 2022.
- [20] Feng Li, Hao Zhang, Shilong Liu, Jian Guo, Lionel M Ni, and Lei Zhang, “Dn-detr: Accelerate detr training by introducing query denoising,” in *Proceedings of the IEEE/CVF Conference on Computer Vision and Pattern Recognition*, 2022, pp. 13619–13627.
- [21] Joao Carreira and Andrew Zisserman, “Quo vadis, action recognition? a new model and the kinetics dataset,” in *proceedings of the IEEE Conference on Computer Vision and Pattern Recognition*, 2017, pp. 6299–6308.
- [22] Jeffrey Pennington, Richard Socher, and Christopher D Manning, “Glove: Global vectors for word representation,” in *Proceedings of the 2014 conference on empirical methods in natural language processing (EMNLP)*, 2014, pp. 1532–1543.
- [23] Adams Wei Yu, David Dohan, Quoc Le, Thang Luong, Rui Zhao, and Kai Chen, “Fast and accurate reading comprehension by combining self-attention and convolution,” in *International conference on learning representations*, 2018, vol. 2.
- [24] Hao Zhang, Aixin Sun, Wei Jing, Liangli Zhen, Joey Tianyi Zhou, and Rick Siow Mong Goh, “Parallel attention network with sequence matching for video grounding,” *arXiv preprint arXiv:2105.08481*, 2021.